Preliminary experiments on high-speed imaging of bubble behaviors during subcooled flow boiling at low and medium pressures

Chanmin Jeong, Ahyeong Cho, Inyeop Kang, Jonghwi Choi, Banseok Bae, Hyungdae Kim*
Department of Nuclear Engineering, Kyung Hee University, Republic of Korea
Corresponding author: hdkims@khu.ac.kr

***Keywords :** Subcooled flow boiling, Medium pressure, High-speed imaging of bubble dynamics*

1. Introduction

Pressurized water reactors (PWRs) operate at 15.5 MPa to remove heat efficiently in the reactor core. Therefore, understanding and accurately predicting subcooled flow boiling on fuel rod surfaces are important for reactor thermal-hydraulic design and safety analysis.

Wall heat-flux partitioning models are widely used to predict heat transfer during subcooled flow boiling by dividing the wall heat flux into different heat-transfer mechanisms. The RPI model decomposes the wall heat flux into three components: single-phase convection, evaporation, and quenching [1]. Gilman and Baglietto proposed a more self-consistent framework by incorporating the effects of microlayer evaporation at the boiling surface and bubble sliding along the heated surface. These models include bubble behavior parameters, such as the bubble departure diameter (D_d), bubble departure frequency (f), and nucleation site density (N''), as key inputs for heat-flux prediction [2]. Because the predicted wall heat flux is sensitive to these parameters, their accurate characterization is essential. In particular, the bubble departure diameter is important because it appears as a cubic term in the evaporation heat-flux calculation, making the predicted heat flux highly sensitive to its value (1). Previous studies have demonstrated a pressure dependence of boiling bubble dynamics, including D_d, f and N'' [3–5]. However, quantitative experimental data at medium pressures or PWRs operating conditions remain relatively limited because visualization and quantitative measurement of bubbles medium pressure flow boiling conditions are technically challenging.

In this study, preliminary observations of bubble behavior especially bubble departure diameter were made during medium pressure subcooled flow boiling simulate PWRs subchannel flow velocity using high-speed video (HSV) camera.

$$q''_e = \frac{1}{6}\pi D_d^3 \rho_g h_f f N'' \quad (1)$$

2. Experimental Setup

2.1 KHU high-pressure flow loop

The high-pressure flow loop at Kyung Hee University (KHU) consists of three main sections: the pressurization loop, the high-pressure loop, and the nitrogen loop (Fig. 1). In the pressurization loop, the deionized (DI) water can be pressurized up to 15.5 MPa at a maximum flow rate of 0.6 LPM. The pressurized water can be heated by a preheater to a maximum temperature of 320°C before being supplied to the agitator tank. In the high-pressure loop, the heated water is delivered to the test section at a constant flow rate, while an impeller installed inside the agitator tank increases the mass flux to a maximum of 3500 kg/m²s. The nitrogen loop supplies nitrogen gas to the test section at a pressure equal to that in the high-pressure loop. A piston accumulator maintains pressure equilibrium between the high-pressure loop and the nitrogen loop, reducing the pressure difference across the test specimen to maintain its integrity.

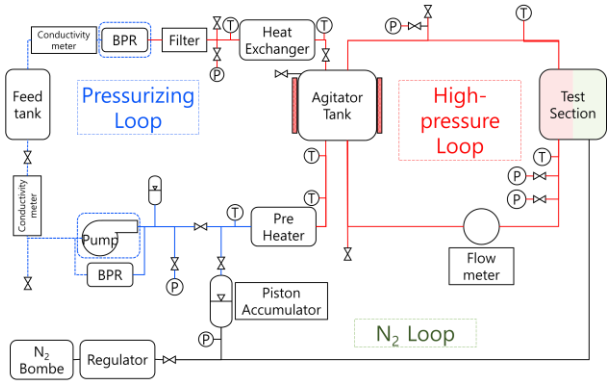

Fig. 1 P&ID of the high-pressure flow loop at KHU

2.2 Test section

The test section consists of three main components: a heater cartridge, a window cartridge, and a main body (Fig. 2). The heater cartridge secures the test specimen and provides electrical connections to the electrodes, enabling the specimen to be heated by Joule heating. The window cartridge is coupled to the heater cartridge to form a 5 mm × 5 mm flow channel and provides a window for visualizing bubble behavior on the test specimen. The test specimen is made of sapphire (15 mm x 15 mm with a thickness of 1 mm) and a CrN–TiN heating film is sputtered onto its upper surface. The heating film has an active heating area of 4 mm × 8 mm. Cr thin-film electrodes are subsequently deposited by 360° rotational sputtering to provide electrical connection from the heating film on the upper surface to the underside of the specimen (Fig. 3). Electrical leads are connected to the electrodes on the underside of the

specimen to supply power to the heating film. The main body is fabricated from stainless steel to withstand high-temperature and high-pressure conditions and contains a rectangular flow passage in which the heater and window cartridges are installed.

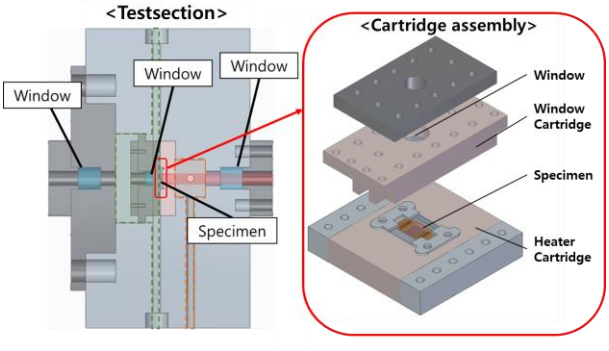

Fig. 2 Schematic diagram of the test section

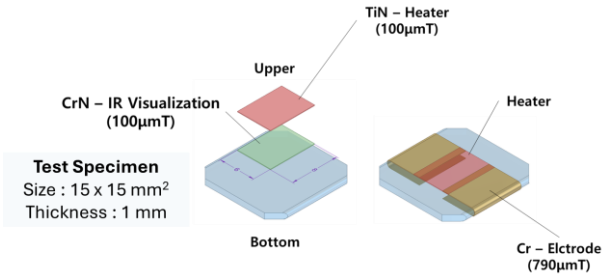

Fig. 3 Schematics of the test specimen

2.3 Optical system

An optical system was constructed to capture the behavior of boiling bubbles generated on the test specimen using HSV (Fig. 4). The system consists of a light source, a 50:50 prism beam splitter, and a HSV. Light from the source passes through the beam splitter and is directed onto the test specimen. The light reflected from the test specimen is then redirected by the beam splitter at a 45° angle toward the HSV camera, enabling high-speed visualization of the boiling bubble behavior.

A Phantom V7.3 HSV camera is used to capture the bubble behavior during the experimental runs. The camera has a maximum image resolution of 800 × 600 pixels and is capable of capturing images at a rate of 6,688 fps at full resolution and up to 500,000 fps at reduced resolution.

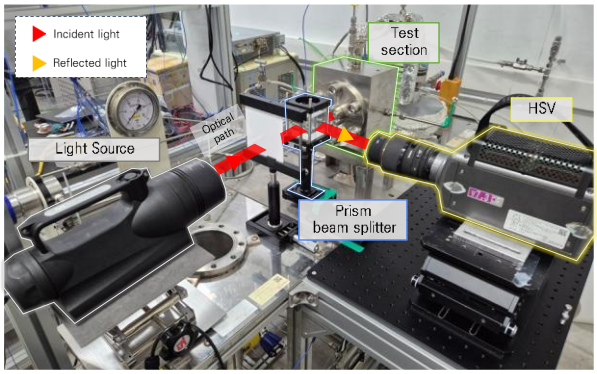

Fig. 4 Overview of HSV optical system

2.4 Experimental conditions

DI water was used as the working fluid. Prior to each experimental run, the water was heated and pressurized until the target pressure and temperature conditions were reached. The experiments were conducted under two operating conditions, as summarized in Table 1. In Case 1, the system pressure, water subcooling, and flow velocity were maintained at 1.3 bar(abs), 17.2 K, and 4.6 m/s, respectively, while the applied wall heat flux was varied from 1610 to 2190 kW/m². In Case 2, the corresponding conditions were 19.7 bar(abs), 19.0 K, and 4.38 m/s, with the wall heat flux varied from 1708 to 2188.4 kW/m². Boiling behavior was recorded for 5 s using a high-speed video camera at 5,000 fps for Case 1 and 2,000 fps for Case 2.

Table.1 Experimental conditions

Condition	Case 1	Case 2
Pressure (bar)	1.3±0.40	19.7±0.14
Water subcooling (K)	17.2±0.085	19.0±0.56
Flow velocity (m/s)	4.60±0.023	4.38±0.78
Wall heat flux (kW/m²)	1610, 1832, 2019, 2190	1708, 1876, 2025, 2188
Frame rate (fps)	5000	2000
Pixel resolution (mm/px)	0.040	0.012
Recording duration (s)	5	5

3. Results and Conclusions

3.1 Results

Subcooled flow boiling experiments were conducted at pressures of 1.3 and 19.7 bar. For each pressure and heat-flux condition, 10 individual bubbles were analyzed, and the mean departure diameter was obtained from these measurements. The observed bubble departure diameter was 0.19 mm at 1.3 bar and decreased to 0.12 mm at 19.7 bar, with an estimated measurement uncertainty of ±0.056 mm. Thus, as the pressure increased from 1.3 to 19.7 bar. Kossolapov et al.

reported a bubble radius of approximately 0.05 mm at 20 bar [6]. In this study, the observed bubble departure radius was approximately 0.06 mm at 19.7 bar. The measured radius is of the same order of magnitude as previously reported high-pressure data. However, direct quantitative comparison is not warranted because the operating conditions and departure definitions differ. Bubble departures were observed at intervals of approximately 0.6 ms at 1.3 bar and 0.5 ms at 19.7 bar (Fig. 5). Figure.6 presents the mean bubble departure diameter as a function of heat flux at 1.3 and 19.7 bar, where each data point represents the mean of 10 individual bubble measurements and the error bars indicate ±1 standard deviation. At a given pressure, D_d increased with increasing heat flux, and this trend was consistently observed at both 1.3 and 19.7 bar. This increase is attributed to the higher wall superheat at higher heat fluxes, which promotes bubble growth and results in a larger departure diameter [7]. A pressure dependence of D_d was also observed: at all heat-flux conditions, D_d measured at 19.7 bar was smaller than that measured at 1.3 bar.

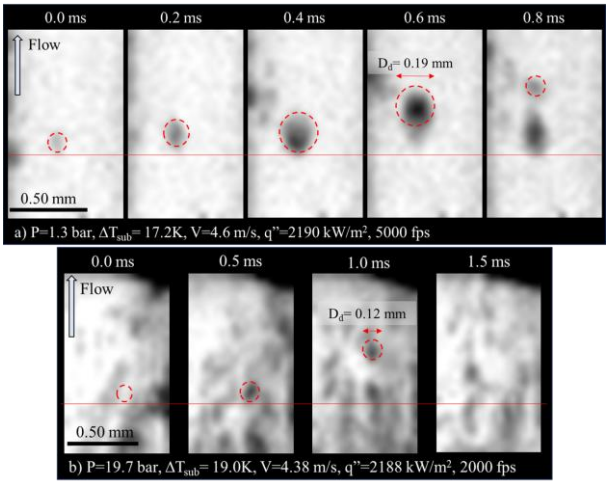

Fig. 5 HSV image of boiling bubble (a) P=1.3 bar, (b) P=19.7 bar

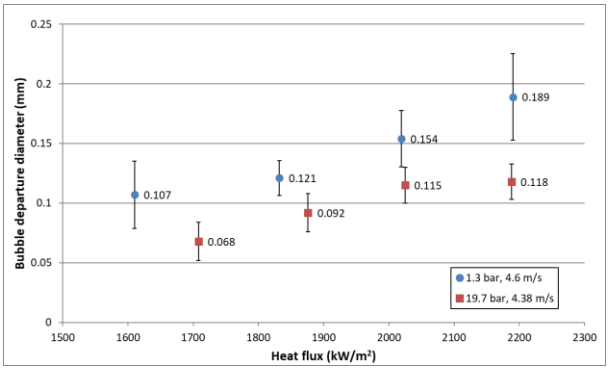

Fig. 6 Bubble departure diameter at different heat fluxes and pressures

3.2 Conclusions and Limitations

A preliminary high-speed visualization study was conducted under pressurized subcooled flow-boiling conditions. The study aimed to establish an experimental framework for investigating boiling phenomena relevant to nuclear reactor thermal-hydraulic safety analysis. The resulting experimental data are also intended to support the validation of subcooled boiling heat-transfer models. Bubble departure behavior was visualized and was observed within the tested conditions The average bubble departure diameter decreased from 0.19 mm at 1.3 bar to 0.12 mm at 19.7 bar. The time intervals between bubble departures were approximately 0.6 ms at 1.3 bar and 0.5 ms at 19.7 bar. The dependence of bubble departure diameter on pressure and heat flux was observed.

The present preliminary experiments were limited by insufficient temporal resolution for detailed analysis of bubble dynamics and by degradation of image quality due to mechanical vibrations transmitted to the optical system. Improvements in the optical setup and imaging conditions are expected to enable more reliable quantitative measurements, less uncertain. Using the experimental framework established in this study, future experiments will investigate bubble dynamics over a wider range of operating pressure, coolant subcooling, flow velocity, and wall heat flux.

The resulting experimental data are expected to provide physical insight into subcooled flow boiling and serve as validation data for the development and assessment of heat-transfer models.

Acknowledgement

This work was supported by the Nuclear Safety Research Program through the Korea Foundation Of Nuclear Safety (KoFONS) using the financial resource granted by the Nuclear Safety and Security Commission (NSSC) of the Republic of Korea. (2106022)
This work was supported by the Korea Institute of Energy Technology Evaluation and Planning (KETEP) and the Ministry of Climate, Energy & Environment (MCEE) of the Republic of Korea (No. RS-2023- 0244330)

REFERENCES

[1] N. Kurul and M. Z. Podowski, On the Modeling of Multidimensional Effects in Boiling Channels, ANS Proceedings of the 27th National Heat Transfer Conference, July 28-31, 1991, Minneapolis, MN.
[2] L. Gilman and E. Baglietto, A Self-Consistent, Physics-Based Boiling Heat Transfer Modeling Framework for Use in Computational Fluid Dynamics, International Journal of Multiphase Flow, Vol. 95, pp. 35-53, 2017.
[3] G. Kocamustafaogullari, Pressure Dependence of Bubble Departure Diameter for Water, International Communications in Heat and Mass Transfer, Vol. 10, pp. 501-509, 1983.
[4] G. Kocamustafaogullari and M. Ishii, Foundation of the Interfacial Area Transport Equation and Its Closure Relations, International Journal of Heat and Mass Transfer, Vol. 38, pp. 481-493, 1995.
[5] H. Sakashita, Bubble Growth Rates and Nucleation Site Densities in Saturated Pool Boiling of Water at High Pressures, Journal of Nuclear Science and Technology, Vol. 48, pp. 734-743, 2011.

[6] A. Kossolapov, M. T. Hughes, B. Phillips, and M. Bucci, Bubble Departure and Sliding in High-Pressure Flow Boiling of Water, Journal of Fluid Mechanics, Vol. 987, p. A35, 2024.
[7] Basu, N., Warrier , G. R., and Dhir, V. K, Wall Heat Flux Partitioning During Subcooled Flow Boiling: Part 1—Model Development, Journal of Heat Transfer, Vol. 127(2), 2005.